Influence of Metallic Interlayers on the Lap Shear Strength of Laser Joined Plastic and Metal Hybrids

Wolfgang Tillmann , Lukas Wojarski , Christian Hopmann , Patricia Fatherazi , Christian Timmer *

Posted Date: 7 December 2023

doi: 10.20944/preprints202312.0483.v1

Keywords: Plastic-metal hybrid; laser joining; Surface free energy; Polyamide 6.6; Polypropylene; AISI 304; Joining process; Dissimilar joining; Arc-PVD; Adhesion

Article

Influence of Metallic Interlayers on the Lap Shear Strength of Laser Joined Plastic and Metal Hybrids

Wolfgang Tillmann [1], Lukas Wojarski [1], Christian Hopmann [2], Patricia Fatherazi [2] and Christian Timmer [1,*]

[1] TU Dortmund University, Institute of Materials Engineering (LWT), Leonhard-Euler-Straße 2, 44227 Dortmund, Germany; office-lwt.mb@tu-dortmund.de

[2] RWTH Aachen, Institute of Plastics Processing in Industry and Craft at RWTH Aachen University (IKV), Seffenter Weg 201, 52074 Aachen, Germany; zentrale@ikv.rwth-aachen.de

* Correspondence: Christian.Timmer@tu-dortmund.de; Tel.: +49 231 755-5681

Abstract: The strength of laser joined metal and plastic hybrids is based purely on adhesion. Unpolar plastics like polypropylene depend solely on the mechanical adhesion while polar plastics like polyamide 6.6 develop covalent bonds with the metal. In this research the influence of different surface metallizations on the lap shear strength of laser joined hybrids was investigated. Sandblasted AISI 304 was used as base metal and reference. Aluminum and titanium coatings were deposited by the means of Arc-PVD. Polypropylene and polyamide 6.6 were utilized as polar und unpolar plastics. The lap shear strength of all hybrids with polyamide 6.6 was higher than the polypropylene samples. For all investigated variations of the laser power, scanning speed and the cohesive and adhesive failure modes, the samples joined with the sandblasted AISI 304 showed the highest lap shear strength. The reduction in lap shear strength for the coated samples was due to the increased difference in thermal conductivity between the plastics and the coating materials. This lead to increased warping and residual stresses. It can be concluded that the thermal properties of the metallization in laser joined metal and plastic hybrids has a high impact on the lap shear strength.

Keywords: plastic-metal hybrid; laser joining; surface free energy; Polyamide 6.6; polypropylene; AISI 304; joining process; dissimilar joining; Arc-PVD; adhesion

1. Introduction

Typical methods for creating metal and plastic hybrids are joining via adhesive, mechanical fasteners, or thermal joining [1]. In comparison with mechanical fastening, no additional weight is added to the component. An advantage over adhesives is, that thermal joining is a very fast joining process without any curing times. Thermal joining is also referred to as direct thermal joining because these processes lack additional components. Different energy sources like ultrasound [2], induction [3] and lasers [4] can be used. Lasers have the advantage of non-contact heat input and a high degree of automatization. The first scientific publication on the utilization of lasers for thermal joining was by Kawahito et al. in the year 2006 [5]. They defined the term laser-assisted metal and plastic (LAMP) joining which was used broadly in the scientific community [6]. The needed temperature to melt the plastic is generated by transmitting the laser through the plastic and heating the interface or by heat transfer through the cross section of the metal. Figure 1 shows a schematic figure of the heat transfer joining also known as indirect LAMP joining [7]. The force is needed to ensure a sufficient pressure that the molten plastic will wet the surface of the metal. The molten plastic will wet the surface and create a bond to the metal. Due to the fundamentally different chemical composition of metals and plastic the bond bases completely on adhesion.

Preprints (www.preprints.org) | NOT PEER-REVIEWED | Posted: 7 December 2023 doi:10.20944/preprints202312.0483.v1

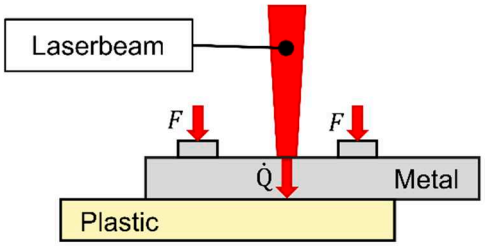

Figure 1. Schematic figure indirect laser assisted metal and plastic (LAMP) joining [7].

Adhesion is a very complex scientific topic. No universal theory has been developed that includes every aspect of adhesion. There are seven common theories of adhesion: Mechanical interlocking, Electric double layer, Adsorption, Diffusion, Chemical Bonding, Acid-Base and Weak boundary layers [8]. In this research the focus is set on the adsorption theory of thermodynamic theory of adhesion and the chemical bonding. The thermodynamic theory of adhesions states, that with higher surface free energy the work of adhesion rises in value [9,10]. In adhesive technology different surface treatments are used to increase the surface free energy like plasma treatments or chemical activation [11]. This results in increased strength of metal and plastic hybrids joined with an adhesive. With optimized treatment parameters a low-pressure plasma treatment can increase the lap shear strength of bonds with polyamide 6.6 (PA6.6) from 1.13 MPa to 6.47 MPa [12]. These treatments can also be used for Metals. A low-pressure plasma treatment of AlMg1SiCu alloys with an oxygen-plasma increase the lap shear strength of bonds from 5.77 MPa to 15.13 MPa created with an adhesive [13]. Laser joined aluminum and PA6.6 samples were treated with a low-pressure plasma prior to joining process. With an increase in surface free energy of either material the maximum shear load rose. It peaked when both materials were treated prior to the joining process indicating a correlation between rising surface free energy and increasing lap shear strength [14]. In a prior research by the authors polyamide 6.6 and polypropylene were treated with different plasma gases to increase the surface free energy and the number of polar groups on the surface. While the surface free energy was significantly increased, the lap shear strength of all investigated samples were lower than the untreated state [7]. This shows, that the correlation between surface free energy and lap shear strength is not clearly identified for laser joined metal and plastic hybrids.

Plastics without unpolar groups like polypropylene (PP) need a surface treatment to ensure mechanical interlocking [5]. Schricker et al. used laser ablation to create the mechanical interlocking increasing the tensile strength from zero to 8.7 MPa [15]. In contrast to that polar plastics can be joined to metals without the need of mechanical interlocking. Katayama et al. joined AISI 304 with a cold rolled surface with polyethylene terephthalate (PET) and achieved shear loads of 3000 N. The plastic and steel surface were bonded through the formation of a chromium oxide layer [16]. Also Liu et al. [17] detected chemical bonds in laser joined aluminum – PA6.6 hybrids. A chemical reaction formed carbon-oxygen-aluminum bonds on the interface between metal and plastic. As possible reaction site is the double oxygen bond of the amide group in PA6.6. This was confirmed by Hirchenhahn et al. [18,19]. Chen et al. developed a new method which combines ultrasound and lasers to create a metal and plastic hybrid [20]. They created sound joints out of titanium (ASTM B265 Grade 1) and PET. At the fractured surface Ti-C, Ti-O and Ti_2O_3 chemical bonds were detected indicating a chemical reaction between plastic and metal [21].

This research focuses on the influence of metal surfaces on the lap shear strength of laser joined plastic and metal hybrids. To minimize the influence of the different thermal properties of the metals thin coatings by the means of arc PVD are used. As coating materials pure aluminum and titanium were used. AISI 304 with a sand blasted surface was used as base to be joined with PA6.6 and PP. PA6.6 was used due to its ability to form covalent bonds with all the different coatings used and PP served as control group to identify possible influences of the thermal conductivity.

Preprints (www.preprints.org) | NOT PEER-REVIEWED | Posted: 7 December 2023 doi:10.20944/preprints202312.0483.v1

2. Materials and Methods

2.1. Materials

The plastics used are polypropylene and polyamide 6.6. As base metal AISI 304 was utilized. Aluminum and titanium were used as different surface metallizations. All samples hat the same geometry of 50 mm x 25 mm x 2 mm. The thermal properties and the tensile strength of the used materials are shown in Table 1.

Table 1. Thermal properties and tensile strength of the materials and coatings used.

Material	Thermal conductivity	Specific heat capacity	Melting range	Tensile Strength	Sources
	[W m^{-1} K^{-1}]	[J kg^{-1} k^{-1}]	[°C]	[MPa]	[-]
AISI 304	15	500	1400 – 1455	540 – 750	[22]
Aluminum	236	520	660	105 – 145	[23–25]
Titanium	22	520	1668	380	[26]
Polypropylene	0,17 – 0,25	2090	160 – 165	35	[27,28]
Polyamide 6.6	0,23 – 0,33	1670	255 – 260	85	[27,29]

To ensure a mechanical interlocking between polypropylene and the metal surface sand blasting was utilized. Table 2 shows the surface roughness of the coated and uncoated AISI 304 samples. The sandblasting also ensured a good adhesion between the steel surface and the coating. For the sandblasting process a SMG 50 of MHG Strahlanlagen was utilized. Corundum with a particle size between 150 and 212 µm was blasted with 4 bar air pressure at an angle of 90° at a distance of 50 mm on the surface of the steel. Only one side of the steel was sandblasted. The arithmetic surface roughness of all samples is within the same category indicating a comparable mechanical interlocking between all samples.

Table 2. Surface roughness of the used samples.

Surface	R_z	
	x [µm]	S [µm]
Sandblasted	14.7	1.7
Sandblasted + Al-coating	13.9	2.0
Sandblasted + Ti-coating	15.7	1.3

The coated samples were manufactured via Arc-PVD. An Interatom PVD 20 of the Interatom GmbH was utilized. Only the sandblasted surface was coated. Five measuring points at three spots of three samples were used to determine the arithmetic mean of the Arc-PVD coatings. The thickness of the samples including the standard deviation is shown in Table 3.

Table 3. Thickness of the applied Arc-PVD coatings.

Coating	Thickness	
	X [µm]	s [µm]
Al	7.9	2.7
Ti	8.7	1.9

2.2. Laser setup

The laser setup described in this chapter was also used in [7]. The fiber laser was an Raycus RFL-QCW150. The laser was used in a CW (continuous wave) mode. A maximum power level of the laser

Preprints (www.preprints.org) | NOT PEER-REVIEWED | Posted: 7 December 2023 doi:10.20944/preprints202312.0483.v1

was 250 W and the used spot diameter was 5 mm. The wavelength of the laser was 1090 nm. Figure 2 shows the CAD generated images of the laser mount and the sample holder.

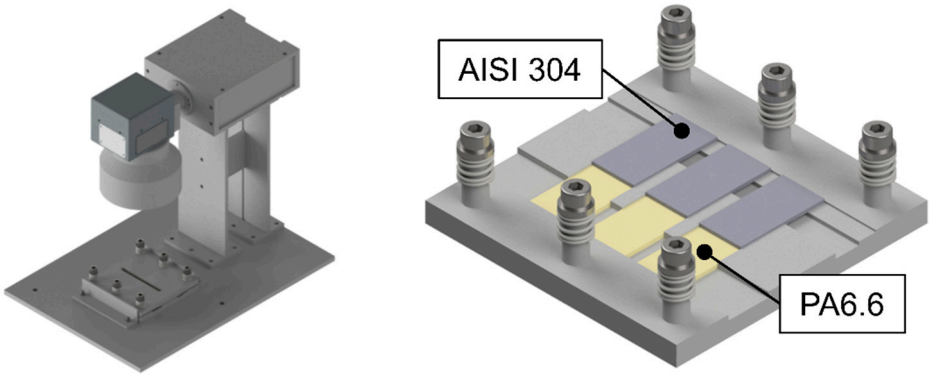

(**a**) (**b**)

Figure 2. CAD generated image of the a) laser mount with sample holder and b) sample holder without the cover plate [7].

Up to three samples can be placed in the sample holder. Six compression springs were used to achieve a uniform pressure level of 0.4 MPa on every sample. In this research different laser power levels and scanning speeds were utilized. To achieve a better comparison with other publications the line energy was calculated by dividing the laser power by the scanning speed. The used parameters are noted in Table 4. The joining parameters for polyamide 6.6 at 237.5 W and 1.5 mm s^{-1} and for polypropylene at 162.5 W and 2 mm s^{-1} were developed in another publication [7]. Additional experiments were conducted to identify parameter sets with the highest lap shear strength without any cohesive failure of the plastic. The laser power and scanning speed were incrementally varied to lower laser powers and scanning speeds. This resulted in two parameter sets at 237.5 W and 2 mm s^{-1} for the Al coated and at 200 W and 2.5 mm s^{-1} for the Ti coated AISI 304 respectively. Additional samples with sandblasted AISI 304 were created as reference at these parameter sets.

Table 4. Used laser powers and scanning speeds.

Plastic	Failure mode [-]	Laser power [W]	Scanning speed [mm s^{-1}]	Line energy [J mm^{-1}]
Polyamide 6.6	Cohesively	237.5	1.5	158
Polypropylene	Adhesively	162.5	2	81
Polyamide 6.6	Adhesively	237.5	2	119
		200	2.5	80

2.3. Contact angle and surface free energy measurement

The surface free energy can be calculated through the contact angle of different measuring liquids and methods. The method by Owens, Wendt, Rabel and Kaelble [30] (OWRK-Method) is frequently used and was also utilized in this research. Based on the formula by Young [9] they used the geometric mean to calculate the overall surface free energy with a dispersive and a polar component.

$$\sigma_l(1+\cos(\theta)) = 2\left(\sqrt{\sigma_s^d \sigma_l^d} + \sqrt{\sigma_s^p \sigma_l^p}\right) \quad (1)$$

While θ is the contact angle between the surface, liquid and atmosphere, σ_l and σ_s are the surface tension of the liquid and surface respectively. The polar and dispersive components are described by the superscripted letters. The contact angles of two different liquids with known surface

Preprints (www.preprints.org) | NOT PEER-REVIEWED | Posted: 7 December 2023 doi:10.20944/preprints202312.0483.v1

tensions are required for the OWRK-method. The two test liquids used in this research and their respective surface tensions summarized in Table 5 [31].

Table 5. Surface tensions of the used test liquids.

Liquid	σ_l [mN m^{-1}]	σ_l^d [mN m^{-1}]	σ_l^p [mN m^{-1}]
Water	72.8	51	21.8
Diiodomethane	50.8	50.8	0

Ten measurements were taken of each sample with each test liquid. 3 µl diiodomethane and 5 µl water were utilized for each respective test. Each measurement was taken on a different location on the tested surface. The contact angel was analyzed with ImageJ and the plugin for contact angels.

2.4. Mechanical testing and microstructural analysis

For mechanical testing of the lap shear force an Instron E10000 with a test speed of 0.5 mm min^{-1} was utilized. To reduce bending stresses spacers with 2 mm thickness were placed below each overlapping side of the sample. The lap shear strength was calculated by dividing the maximal shear force with the wetted area. The wetted area was identified with a macroscopic image of the joined zone taken with a Canon EOS 600D for each sample individually. ImageJ was utilized to measure the wetted area of all samples. For each parameter set 5 lap shear samples were tested. Also every failed sample was investigated macroscopically.

3. Results and Discussion

3.1. Cohesively failed samples

This subsection includes the samples joined between the different metal surfaces and polyamide 6.6 which failed cohesively in the plastic itself. Figure 3 shows the samples in the as-joined state in the top-row while the bottom row shows them after the lap shear test.

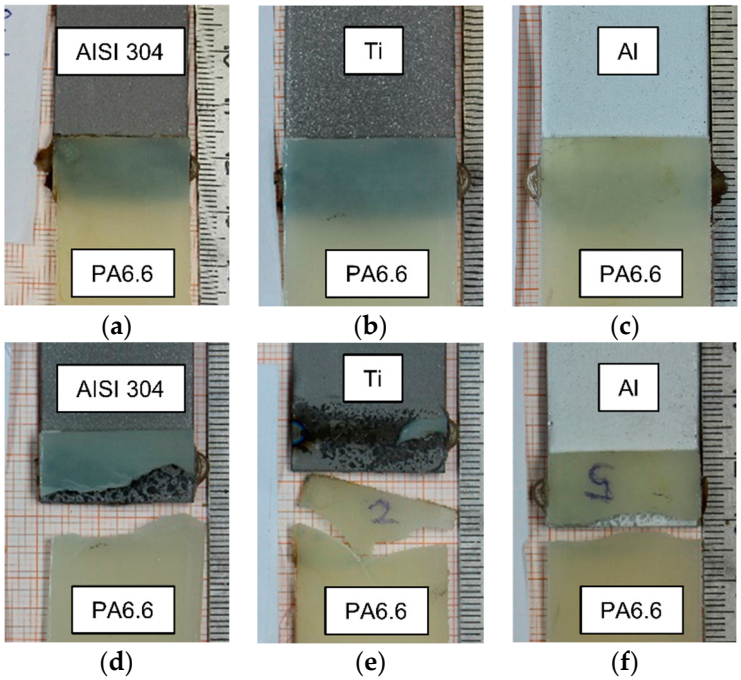

Figure 3. Hybrids joined with polyamide 6.6 and (**a**) AISI 304, (**b**) Ti, (**c**) Al and the same samples after lap shear testing in (**d**), (**e**) and (**f**) which failed cohesively.

Preprints (www.preprints.org) | NOT PEER-REVIEWED | Posted: 7 December 2023 doi:10.20944/preprints202312.0483.v1

Every sample tested at this parameter set failed cohesively in the plastic. Plastic residue is visible on every metal surface. This indicates covalent bonds between the polyamide 6.6 and every metallization used. In Figure 3 (**d**) and (**f**) the second half of the polyamide 6.6 is still bonded to the metal while in Figure 3 (**e**) the second half broke off. These two types of cohesive failure modes occurred randomly for every investigated surface metallization. Figure 4 shows the measured lap shear strength of the cohesively failed samples.

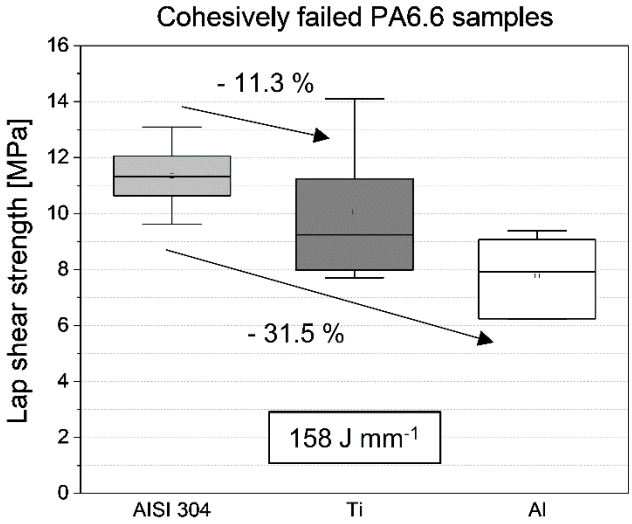

Figure 4. Lap shear strength of the cohesively failed polyamide 6.6 hybrids.

The uncoated and sandblasted AISI 304 polyamide 6.6 hybrids showed the highest lap shear strength at an arithmetic mean of 11.3 MPA. It should be mentioned, that the range of measured values of hybrids with sandblasted AISI 304 is on the same level as for cold-rolled AISI 304 and polyamide 6.6 samples investigated in an earlier work on this subject [7]. 10.05 MPa is the arithmetic mean of the Ti-coated samples which is 11.3 % lower in comparison to the uncoated samples. The reduction in strength of the Al-coated samples was even higher. The arithmetic mean was 7.77 MPa which is 31.5 % lower than the uncoated samples. It should be mentioned that the deviation of values of the Ti-coated samples is significantly higher than the other investigated coatings. The highest absolute value exceeds the measured lap shear strengths of the uncoated samples. Nonetheless, the trend is clear, that the different surface metallization reduces the lap shear strength. The thermal properties are shown in Table 1. The thermal conductivity for Ti is higher and significantly higher for Al in comparison with the base material. But the influence of the different covalent bonds due to the different metallization and the influence of the cohesive failure mode on the lap shear strength is not clear. Due to these points the experiments with polypropylene were carried out, due to the unpolar nature of this plastic. No covalent bonds are created between unpolar plastics and metals during the thermal joining. Additionally, samples with polyamide 6.6 were created with an adhesive failure mode.

3.2. Adhesively failed samples

Figure 5 shows the laser joined hybrids with polypropylene. As before the top row is in the as-joined state while the top row is after the lap shear test. It should be mentioned that the failed polypropylene hybrid with the Al-coating shown in Figure 5 (**f**) failed before the lap shear test could occur. Every sample failed before they could be tested resulting in a lap shear strength of zero shown in Figure 6.

Preprints (www.preprints.org) | NOT PEER-REVIEWED | Posted: 7 December 2023 doi:10.20944/preprints202312.0483.v1

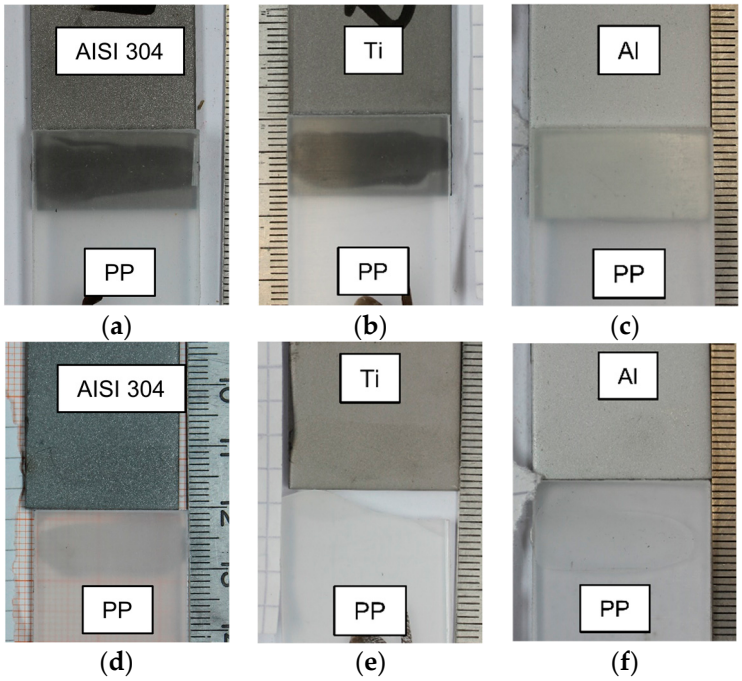

Figure 5. Hybrids joined with polypropylene and (**a**) AISI 304, (**b**) Ti, (**c**) Al and the same samples after lap shear testing in (**d**), (**e**) and (**f**).

In Figure 5 (**a**) and (**b**) the wetted area of the samples is visible as darker area. No equivalent area is visible in Figure 6 (**c**) for the Al-coated sample. In Figure 6 (**f**) it is clearly seen that the energy input plasticized the PP side of the joint. It is possible, that due to high residual stresses the joint detached. During the testing of the Ti-coated sample shown in Figure 5 (**e**) one edge of the polypropylene chipped off. The failure mode was adhesively nonetheless but the high input of thermal energy seems to have introduced high residual stresses, which could lead to this effect. There was no plastic residue on every of the tested polypropylene samples. This confirms the findings shown in the introduction that no covalent bonds are created during the laser joining with polypropylene. In Figure 6 the lap shear strength of the laser joined hybrids with polypropylene is displayed.

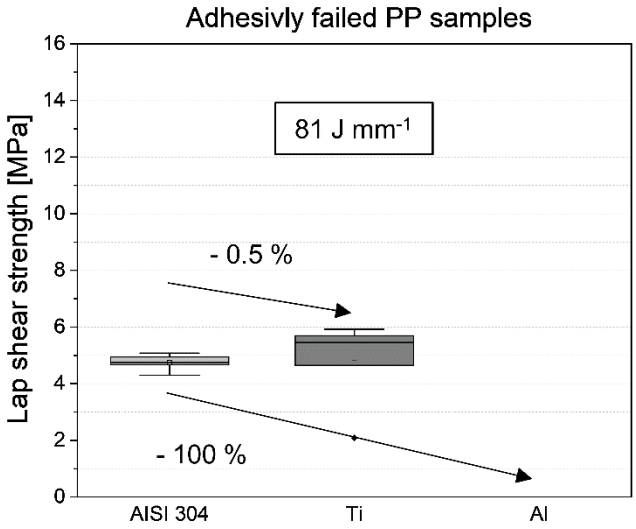

Figure 6. Lap shear strength of the adhesively failed polypropylene hybrids.

In comparison to the hybrids with polyamide 6.6 two things are clearly visible. The Al-coated samples failed all before testing resulting in a lap shear strength of zero and the overall values of the

Preprints (www.preprints.org) | NOT PEER-REVIEWED | Posted: 7 December 2023 doi:10.20944/preprints202312.0483.v1

lap shear strength are significantly lower. The arithmetic mean of the Ti-coated samples is 4.75 MPa which is only 0.5 % less than the arithmetic mean of the sandblasted AISI 304 hybrids with 4.78 MPa. In comparison with the polyamide 6.6 samples the reduction in lap shear strength can be neglected. One of the tested Ti-coated samples had a reduced value of 2.08 MPa. This value leads to a significant reduction of the arithmetic mean. If this sample would be viewed as an outline the arithmetic mean would rise to a value of 5.43 MPa exceeding the sandblasted AISI 304 samples by 16.4 %. For polypropylene it seems that the thermal conductivity plays a role, as seen with the Al-coated samples, but the variation between AISI 304 and the Ti-coating can be neglected.

Furthermore, additional laser joined hybrids with polyamide 6.6 were investigated which showed only an adhesive failure mode. Figure 10 shows the parameter sets which showed the maximum lap shear strength with adhesive failure mode for Al-coated samples at 119 J mm^{-1} and for the Ti-coated samples at 80 J mm^{-1}. Figure 7 has the same pattern as Figure 3 and Figure 5. The top row shows the as-joined state while the lower row shows the tested samples.

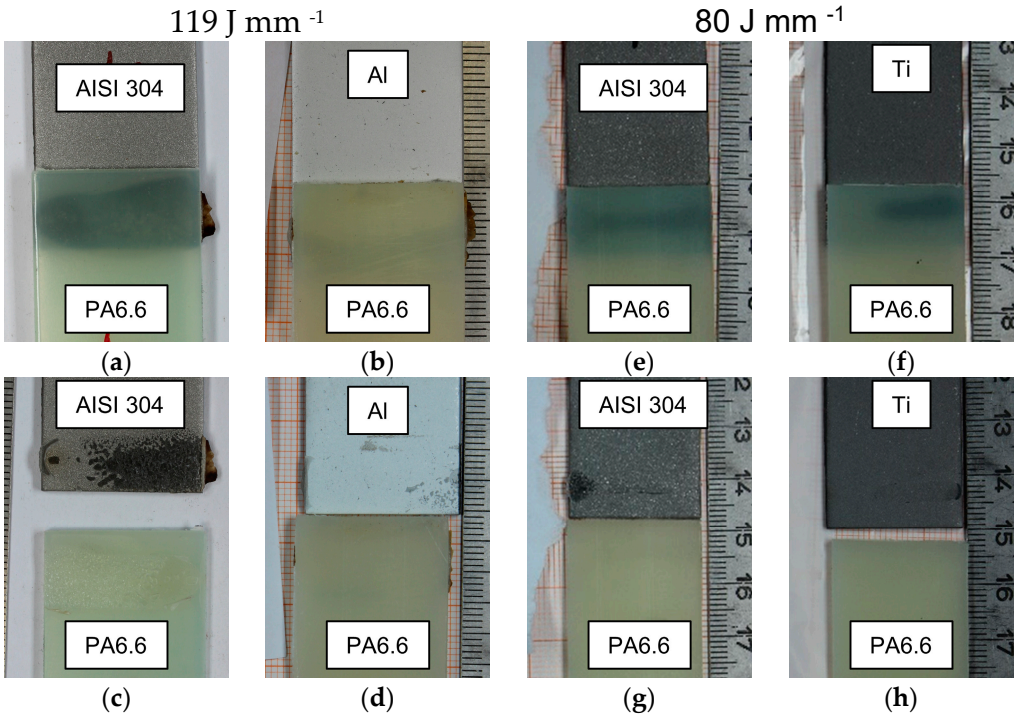

Figure 7. Adhesively failed hybrid joints with polyamide 6.6 joined at 119 J mm^{-1} with (**a**) AISI 304 and (**b**) Al and the same samples after lap shear testing in (**c**) and (**d**) and hybrids joined at 80 J mm^{-1} with (**e**) AISI 304 and (**f**) Ti and the same samples after lap shear testing in (**g**) and (**h**).

The samples joined with 119 J mm^{-1} show a significant difference in the joined area. This is also visible in the amount of residue shown on the metal side of the lap sheared samples shown in Figure 7 (**c**) and (**d**). On the other hand, at 80 J mm^{-1} the joined area is almost identical while the resulting plastic residue is a slightly higher on the AISI 304 lap sheared sample shown in Figure 7 (**g**). The resulting lap shear strength is noted in Figure 8.

Preprints (www.preprints.org) | NOT PEER-REVIEWED | Posted: 7 December 2023 doi:10.20944/preprints202312.0483.v1

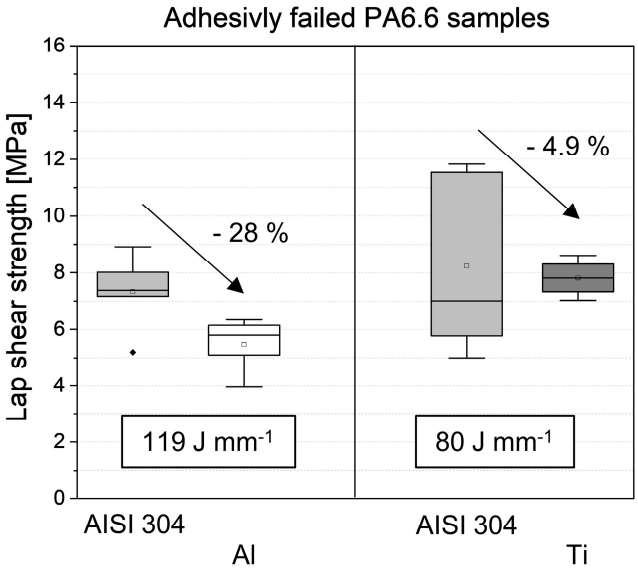

Figure 8. Lap shear strength of the adhesively failed polyamide 6.6 hybrids.

At 119 J mm^{-1} the Al-coated samples achieved an arithmetic mean of 5.3 MPa which was 28 % lower than the reference AISI 304 hybrids with 7.4 MPa. Also the Ti-coated samples joined at 80 J mm^{-1} showed a lower arithmetic mean as the AISI 304 reference. The arithmetic mean of 7.8 MPa is 4.9 % lower than the 8.2 MPa of the AISI 304 reference samples. Both investigated cases show the same behavior as the cohesively failed hybrid joints. The overall level of strength is reduced, but both coatings resulted in a reduced shear strength. The adhesively failed hybrids with polyamide 6.6 show the same trends as the cohesively failed samples as well as the polypropylene hybrids.

3.3. Surface free energy

As mentioned in the introduction, the level of the surface free energy, especially the polar component, is related with the lap shear strength. Within the research about laser joined hybrids the correlation between the surface free energy and the lap shear strength is not clear. The measured values of the surface free energy are displayed in Figure 9 and noted in Table 6.

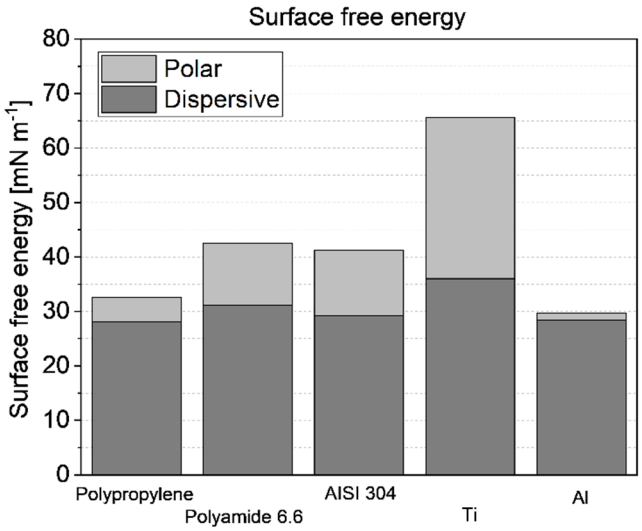

Figure 9. Surface free energy determined by the OWRK-Method.

Comparing the two plastics used in this research, polyamide 6.6 has a significant higher polar and total value than polypropylene. The Ti coated samples have the highest dispersive and polar

 doi:10.20944/preprints202312.0483.v1

values of all investigated surfaces. It has also to be mentioned, that the Al coating has a lower polar component than polypropylene which is considered an unpolar plastic. Taking the lap shear strength in relation, all AISI 304 samples had higher lap shear strength than the Ti coated samples. There is no clear correlation between the surface free energy and the lap shear strength in this research.

Table 6. Surface free energy values shown in Figure 9.

Sample	Dispersive [mN m^{-1}]	Polar [mN m^{-1}]	Total [mN m^{-1}]
Polypropylene	28.05	4.52	32.56
Polyamide 6.6	31.12	11.35	42.47
AISI 304	29.22	12.05	29.68
Ti	36.02	29.51	65.53
Al	28.41	1.27	29.68

3.4. Warp

As mentioned before, the thermal conductivity of the metallization varies significantly. Especially Al has a significant higher thermal conductivity up to a factor of 1000 than the plastics used in this research. This and the fast energy input of the laser joining process can lead to significant residual stresses and warping in the resulting hybrid joint. Figure 10 shows an example of the cohesively failed samples of an Al-coated AISI 304 with polyamide 6.6. The warping is macroscopically visible with a few millimeters. This also indicates that the thermal properties and the resulting residual stresses are more significant in the hybrid joining process than the surface metallization.

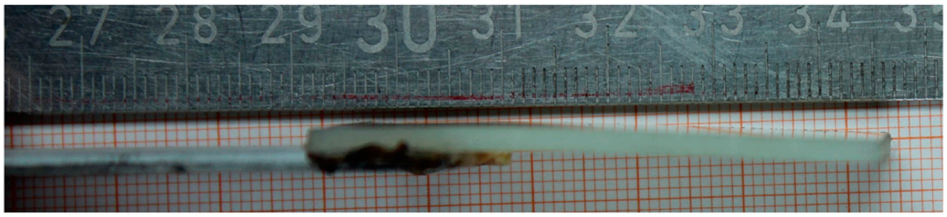

Figure 10. Macroscopic warp of an Al-polyamide 6.6 hybrid joined at 158 J mm^{-1}.

4. Conclusions

In this investigation the influence of different surface metallizations on the lap shear strength of laser joined metal and plastic hybrids is analyzed. Within this research different conclusions could be drawn:

- There was no correlation or trend between the surface free energy of the used samples and the resulting lap shear strength.
- Hybrids with the polar polyamide 6.6 showed higher lap shear strength values as hybrids with polypropylene. This is attributed to covalent bonds between polyamide 6.6 and the metal surface visible by plastic residue on the lap sheared metal surface.
- At every investigated parameter set either with polyamide 6.6 or polypropylene the sandblasted AISI 304 samples showed the highest lap shear strength values in comparison with the Ti and Al coatings. The loss in lap shear strength of the Ti and Al coatings in comparison the with the AISI 304 hybrids are due to the higher thermal conductivity.
- The trend that higher thermal conductivity leads to a lower lap shear strength is true for adhesive and cohesive failure modes for samples joined with polyamide 6.6
- Sound joints with polypropylene and Al coated AISI 304 samples could be achieved but they failed before testing. This can be attributed to very high residual stresses due to the difference in thermal conductivity by factor 1000.

Author Contributions: Conceptualization, W.T., L.W. and C.T.; methodology, C.T.; validation, C.T. and L.W.; formal analysis, C.T.; data curation, C.T.; writing—original draft preparation, C.T.; writing—review and editing,

W.T., L.W. and P.F.; visualization, C.T.; supervision, C.H. and W.T.; project administration, W.T.; funding acquisition, C.H. and W.T.. All authors have read and agreed to the published version of the manuscript.

Funding: This research was funded by the German Research Foundation (DFG, TI 343/170-1, HO 4776/56-1).

Informed Consent Statement: Not applicable.

Data Availability Statement: Not applicable.

Acknowledgments: Not applicable.

Conflicts of Interest: The authors declare no conflict of interest.

References

1. Amancio-Filho, S.T.; dos Santos, J.F. Joining of polymers and polymer-metal hybrid structures: Recent developments and trends. *Polym Eng Sci* **2009**, *49*, 1461–1476, doi:10.1002/pen.21424.
2. Al-Obaidi, A.; Majewski, C. Ultrasonic Welding of Polymer–Metal Hybrid Joints. In *Transactions on Intelligent Welding Manufacturing*; Chen, S., Zhang, Y., Feng, Z., Eds.; Springer Singapore: Singapore, 2019; pp 21–38, ISBN 978-981-13-3650-8.
3. Nagarajan, B.M.; Manoharan, M. Assessment of dissimilar joining between metal and polymer hybrid structure with different joining processes. *Journal of Thermoplastic Composite Materials* **2023**, *36*, 2169–2211, doi:10.1177/08927057211048534.
4. Tillmann, W.; Elrefaey, A.; Wojarski, L. Toward process optimization in laser welding of metal to polymer. Prozessoptimierung beim Laserstrahlschweißen von Metall mit Kunststoff. *Mat.-wiss. u. Werkstofftech.* **2010**, *41*, 879–883, doi:10.1002/mawe.201000674.
5. Kawahito, Y.; Tange, A.; Kubota, S.; Katayama, S. Development of direct laser joining for metal and plastic. In *International Congress on Applications of Lasers & Electro-Optics*. ICALEO® 2006: 25th International Congress on Laser Materials Processing and Laser Microfabrication, Scottsdale, Arizona, USA, October 30–November 2, 2006; Laser Institute of America, 2006; p 604, ISBN 978-0-912035-85-7.
6. Niwa, Y.; Kawahito, Y.; Kubota, S.; Katayama, S. Evolution of LAMP joining to dissimilar metal welding. In *International Congress on Applications of Lasers & Electro-Optics*. ICALEO® 2008: 27th International Congress on Laser Materials Processing, Laser Microprocessing and Nanomanufacturing, Temecula, California, USA, October 20–23, 2008; Laser Institute of America, 2008; p 606.
7. Tillmann, W.; Wojarski, L.; Hopmann, C.; Fatherazi, P.; Timmer, C. *Influence of Low-Pressure Plasma Treatments on the Lap-Shear Strength of Laser Joined AISI 304 Hybrids with Polypropylene and Polyamide 6.6*, 2023.
8. Gardner, D.J. Theories and mechanisms of adhesion. In *Handbook of adhesive technology*, Third edition; Pizzi, A., Mittal, K.L., Eds.; CRC Press: Boca Raton, 2018; pp 3–18, ISBN 9781351637763.
9. Young, T. III. An essay on the cohesion of fluids. *Phil. Trans. R. Soc.* **1805**, *95*, 65–87, doi:10.1098/rstl.1805.0005.
10. Padday, J.F. Contact Angle. In *Handbook of adhesion*, 2. ed.; Packham, D.E., Ed.; Wiley: Chichester, 2005; pp 79–81, ISBN 9780470014226.
11. Liston, E.M.; Martinu, L.; Wertheimer, M.R. Plasma surface modification of polymers for improved adhesion: a critical review. *Journal of adhesion science and technology* **1993**, *7*, 1091–1127, doi:10.1163/156856193X00600.
12. Mandolfino, C.; Lertora, E.; Gambaro, C. Influence of cold plasma treatment parameters on the mechanical properties of polyamide homogeneous bonded joints. *Surface and Coatings Technology* **2017**, *313*, 222–229, doi:10.1016/j.surfcoat.2017.01.071.
13. Mandolfino, C.; Lertora, E.; Genna, S.; Leone, C.; Gambaro, C. Effect of Laser and Plasma Surface Cleaning on Mechanical Properties of Adhesive Bonded Joints. *Procedia CIRP* **2015**, *33*, 458–463, doi:10.1016/j.procir.2015.06.054.
14. Al Sayyad, A.; Bardon, J.; Hirchenhahn, P.; Mertz, G.; Haouari, C.; Laurent, H.; Plapper, P. Influence of laser ablation and plasma surface treatment on the joint strength of laser welded aluminum-polyamide assemblies **2017**.
15. Schricker, K.; Samfaß, L.; Grätzel, M.; Ecke, G.; Bergmann, J.P. Bonding mechanisms in laser-assisted joining of metal-polymer composites. *Journal of Advanced Joining Processes* **2020**, *1*, 100008, doi:10.1016/j.jajp.2020.100008.

16. Katayama, S.; Kawahito, Y. Laser direct joining of metal and plastic. *Scripta Materialia* **2008**, *59*, 1247–1250, doi:10.1016/j.scriptamat.2008.08.026.
17. Liu, F.C.; Dong, P.; Lu, W.; Sun, K. On formation of Al O C bonds at aluminum/polyamide joint interface. *Applied Surface Science* **2019**, *466*, 202–209, doi:10.1016/j.apsusc.2018.10.024.
18. Hirchenhahn, P.; Al Sayyad, A.; Bardon, J.; Felten, A.; Plapper, P.; Houssiau, L. Highlighting Chemical Bonding between Nylon-6.6 and the Native Oxide from an Aluminum Sheet Assembled by Laser Welding. *ACS Appl. Polym. Mater.* **2020**, *2*, 2517–2527, doi:10.1021/acsapm.0c00015.
19. Hirchenhahn, P.; Al-Sayyad, A.; Bardon, J.; Plapper, P.; Houssiau, L. Binding Mechanisms Between Laser-Welded Polyamide-6.6 and Native Aluminum Oxide. *ACS Omega* **2021**, *6*, 33482–33497, doi:10.1021/acsomega.1c04264.
20. Chen, Y.J.; Yue, T.M.; Guo, Z.N. A new laser joining technology for direct-bonding of metals and plastics. *Materials & Design* **2016**, *110*, 775–781, doi:10.1016/j.matdes.2016.08.018.
21. Chen, Y.J.; Yue, T.M.; Guo, Z.N. Fatigue behaviour of titanium/PET joints formed by ultrasound-aided laser welding. *Journal of Manufacturing Processes* **2018**, *31*, 356–363, doi:10.1016/j.jmapro.2017.11.027.
22. Weltstahl. DIN EN Werkstoff 1.4301 Edelstahl X5CrNi18-10 V2A Datenblatt, Zugfestigkeit, Magnetisch, Dichte, Härten. Available online: https://www.weltstahl.com/en-werkstoff-1-4301-edelstahl-x5crni18-10/ (accessed on 10 October 2023).
23. *VDI-Wärmeatlas*: *Mit 320 Tabellen;* VDI-Gesellschaft Verfahrenstechnik und Chemieingenieurwesen, 11., bearb. und erw. Aufl.; Springer Vieweg: Berlin, Heidelberg, 2013, ISBN 978-3-642-19981-3.
24. Batz Burgel. EN AW-1050A (Al 99,5 - 3.0255). EN AW-1050A (Al 99,5 - 3.0255). Available online: https://batz-burgel.com/metallhandel/lieferant-aluminium/en-aw-1050/ (accessed on 10 October 2023).
25. Sturgeon, J.B.; Laird, B.B. Adjusting the melting point of a model system via Gibbs-Duhem integration: Application to a model of aluminum. *Phys. Rev. B* **2000**, *62*, 14720–14727, doi:10.1103/PhysRevB.62.14720.
26. Material properties. What is Titanium – Properties of Titanium Element – Symbol Ti. Available online: https://material-properties.org/pure-titanium-density-strength-hardness-melting-point/ (accessed on 10 October 2023).
27. Schricker, K. Charakterisierung der Fügezone von laserbasiert gefügten Hybridverbunden aus teilkristallinen thermoplastischen Kunststoffen und Metallen. Dissertation; Technische Universität Ilmenau; Universitätsverlag Ilmenau, Ilmenau, 2018.
28. Amend, P. Laserbasiertes Schmelzkleben von Thermoplasten mit Metallen; Friedrich-Alexander-Universität Erlangen-Nürnberg, Erlangen, 2020.
29. Flock, D. Wärmeleitungsfügen hybrider Kunststoff-Metall-Verbindungen; RWTH Aachen, Aachen, 2011.
30. Owens, D.K.; Wendt, R.C. Estimation of the surface free energy of polymers. *J. Appl. Polym. Sci.* **1969**, *13*, 1741–1747, doi:10.1002/app.1969.070130815.
31. Awaja, F.; Gilbert, M.; Kelly, G.; Fox, B.; Pigram, P.J. Adhesion of polymers. *Progress in Polymer Science* **2009**, *34*, 948–968, doi:10.1016/j.progpolymsci.2009.04.007.